Int. J. Electrochem. Sci., 15 **(2020)** 4056 – 4064, doi: 10.20964/2020.05.59

International Journal of
ELECTROCHEMICAL
SCIENCE
www.electrochemsci.org

Photoelectrochemical and Optical Properties of ZnO Nanorods Grown on ITO/polyethersulphone Polymer Substrates Using Aqueous Solution Method: The Effect of Precursor Concentration

Yuqin Jing

School of Electronic Information Engineering, Chong Qing Technology and Business Institute, Chongqing 401520, China
E-mail: yuqinjing_cq@163.com

Received: 12 November 2019 / *Accepted:* 7 February 2020 / *Published:* 10 April 2020

Well-aligned ZnO nanostructures were successfully grown on indium tin oxide (ITO)/ polyethersulphone (PES) polymer substrates using aqueous solution method to study the precursor concentration effect on photoelectrochemical and optical properties of prepared samples. Field-emission scanning electron microscopy (FESEM) was used to characterize the surface morphology of the samples. Photoelectrochemical and optical properties of ZnO nanorods were done by UV–vis spectrophotometer, photoluminescence (PL) and solar simulator tests. The FESEM images demonstrated that smaller diameter and higher-density distribution of ZnO nanorods were observed in the sample with 0.06 M precursor concentration. The optical absorption revealed that the sample with 0.06 M precursor content indicated strangely improved absorption compared to the other samples which can be ascribed to the aspect ratio of the ZnO nanostructures. The PL measurements of the samples demonstrated a strong and sharp enhancement in UV emission peak at a low concentration (0.06 M) of precursor. Photoelectrochemical performance revealed that a proper amount of precursor significantly improve the conversion efficiency and short current density values compared to that of high amount of precursor which can be attributed to the sufficient light harvesting, more dye absorption and fast charge transfer of the sample.

Keywords: ZnO nanorods; Polyethersulphone polymer substrate; Aqueous solution method; Photoelectrochemical and optical properties; Precursor concentration

1. INTRODUCTION

One-dimensional semiconductor nanorods and nanowires have attracted considerable increasing interest because of their physical and structural properties in potential photonic and electronic device

applications [1, 2]. Zinc oxide (ZnO) nanostructures have been widely studied in applications such as gas sensors, ultraviolet nanolaser sources, field emission display devices, and solar cells due to high exciton binding energy and large direct band-gap energy [3-5]. Furthermore, ZnO nanorods have unique advantages including nontoxicity, high specific surface area, chemical stability, high electron communication and electrochemical activityfeatures.

Gas-phase deposition techniques for example chemical vapor deposition are one of the main technologies for the synthesis of highly well-aligned ZnO nanostructures [6]. Although this approach can prepare high-quality aligned ZnO nanorod arrays, it needs metal catalyst particles and high temperature to grow nanostructures [7]. Furthermore, these techniques consume a great deal of energy and require advanced equipment with difficult experimental conditions [8, 9]. Hence, such limitations lead researchers to solution-phase synthesis, which exhibits a new challenge for a large-scale and low-cost fabrication [10]. The low-temperature solution techniques are principally attractive due to their low energy consumption, and environmentally safe synthesis conditions [11].

Compared to paper, glass and silicon substrates, the polyethersulphone (PES) polymer substrates have the benefits of low cost, good flexibility, and high transparency [12]. Large area polymer substrates are commercially available, which are a good alternative substrate for the production of flexible solar cells [13]. Although the aqueous solution technique for growing metal-oxide semiconductor nanostructures have many advantages, no study has been conducted on the preparation of high-quality ZnO nanorod arrays on flexible polymer substrates with the use of this approach. In this study, the well-aligned ZnO nanorods were grown on ITO/PES substrates via an aqueous solution technique. The morphological and structural properties of ZnO nanorods and their photoelectrochemical and optical properties were investigated.

2. MATERIALS AND METHOD

Indium tin oxide (ITO) layer with 150 nm thickness were deposited on polyethersulphone (PES) polymer substrates by pulsed laser deposition method. Well-aligned ZnO nanorods were synthesized on ITO/PES polymer substrates using the aqueous solution technique. Before synthesis process, radiofrequency magnetron sputtering was utilized for deposition of ZnO seed-layer on the substrates. Sputtering was done at 100 W incident power at 100°C for 1 h using a 99.99% purity ceramic ZnO target. Zinc nitrate hexahydrate (with Sample A=0.03 M, Sample B=0.06 M, Sample C=0.1 M, and Sample D=0.15 M concentrations) as precursor and hexamethylenetetramine were separately dissolved in the DI water at the same molar concentrations at ambient temperature. After uniform mechanical mixing and stirring, the ZnO seed-layer/ITO/PES substrates were dipped into the aqueous solution. Operating temperature and growth time were kept at 3 h and 110°C, respectively. Finally, the samples were constantly washed with DI water to eliminate possible impurities and dried.

The photoelectrochemical performances were done by immersing the ZnO/ITO/PES films in the dye bath including (0.1 mM) C218 dye into a solvent mixture of butanol and acetonitrile (1:1, v/v) for 1 hour. (1 mM) co-adsorbent 3α-7α-dihydroxy-5β-cholic acid was added into the dye solution to decrease the dye aggregation Influence on the ZnO/ITO/PES substrates. The sensitized samples were assembled

by a platinum-coated ITO counter electrode, and Surlyn film with a 25 μm thickness was used to control the gap between electrodes. An electrolyte solution drop including 0.2 M NaI, 0.06 M I_2, 0.5 M 4-*tert*-butylpyridine, 0.6 M 1-propyl-3-methylimidazolium iodide and in 3-methoxypropionitrile was added into the gap.

Field-emission scanning electron microscopy were used to characterize the surface morphology of the samples. High-resolution transmission electron microscopy (HRTEM) (TECNAI G2 20S-TWIN, FEI) was employed to characterize the size, morphology, and structure of the ZnO nanorods. The phase and crystallinity of the nanostructures were determined using an X-ray diffractometer (PANalytical, X'Pert PRO). The optical absorption of the samples were done by a UV–vis spectrophotometer. Photoluminescence (PL) spectra were studied by fluorescence spectrophotometer with a 320 nm excitation wavelength at room temperature. The photovoltaic characteristics of the dye-sensitized solar cells (DSSCs**)** were considered by a Solar Simulator under with a 100 mW/cm^{2}xenon lamp power supply (as simulated solar light).

3. RESULTS AND DISCUSSION

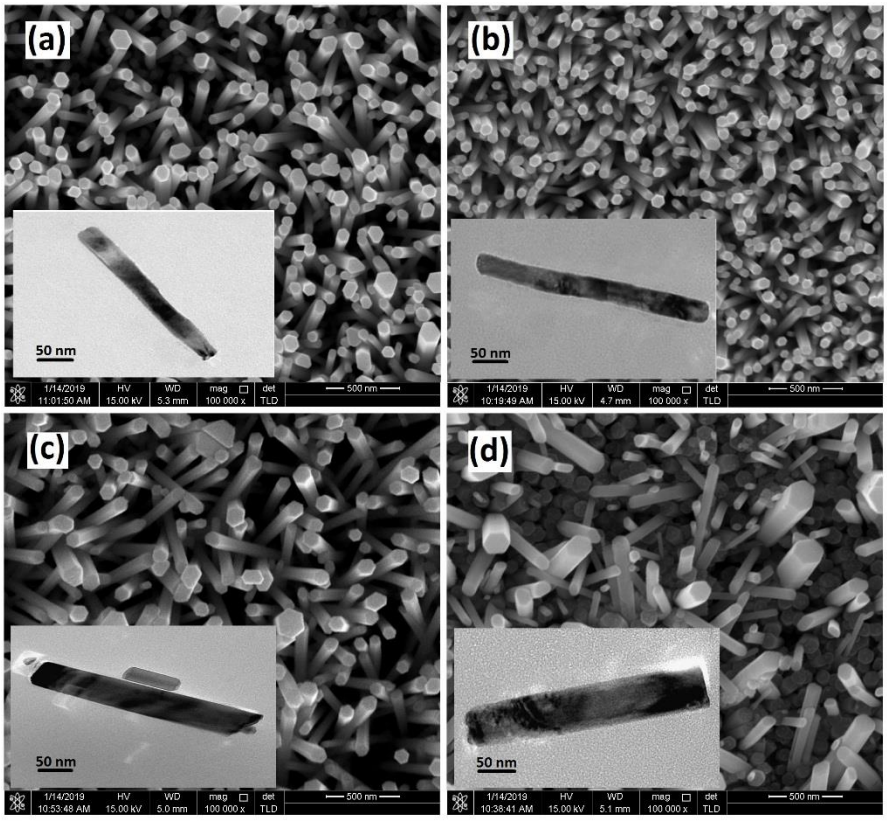

Figure 1. FESEM and HRTEM images of well aligned ZnO nanostructures synthesized on the ITO/PES polymer substrates using different concentrations of precursor (a) 0.03 M (b) 0.06 M (c) 0.1 M (b) 0.15 M

Figure 1 shows the surface morphologies of well aligned ZnO nanostructures synthesized on the ITO/PES polymer substrates using different concentrations of precursor with 3 hours growth time and 110 °C operating temperature. The FESEM images reveal that the samples have hexagonal wurtzite-structure and a high-density ZnO nanorods on the whole surface of substrate. As shown in figure 1b, smaller diameter and higher-density distribution of ZnO nanorods is observed in the sample B. The ZnO production process consists of two stages; First, Zn^{2+} and OH^-ions are produced by the reaction of solution mixture in the aqueous solution process. Then, $Zn(OH_2)$ clusters are produced by the reaction between Zn^{2+} and OH^- ions. The hydrothermal reaction to grow ZnO nanorods are inferred as follows [14]:

$$Zn^{2+} + 2OH^- \leftrightarrow Zn(OH_2) \quad (1)$$

$$Zn(OH_2) \rightarrow ZnO + H_2O \quad (2)$$

Generally, by increasing the precursor concentrations, the value of colloidal zinc hydroxide clusters increases which accelerates the ZnO growth during synthesis process [15]. These chemical reactions are endothermic and may prolong the synthesis of ZnO nanorods in the direction of [001]. Therefore, ZnO nanorods with larger diameter were formed in a higher concentration of precursor. Polsongkram et al. considered the effect of temperature, growth time, and $[Zn^{2+}]$ concentration on the ZnO nanorod morphology and found that the morphology and size of ZnO nanostructures strongly depend on concentration of Zn^{2+} ions [16, 17].

According to TEM micrographs, the size of ZnO nanorods with different concentrations of precursor are completely consistent with the SEM observations. All samples show clean and smooth surfaces. The aspect ratio of the sample B was 10.54 which is significantly higher than the other samples and comparable with other previous studies (Fig. 1). The small-diameter ZnO nanorods may be studied as a new challenge which can be the optimum indicator for suitable growth.

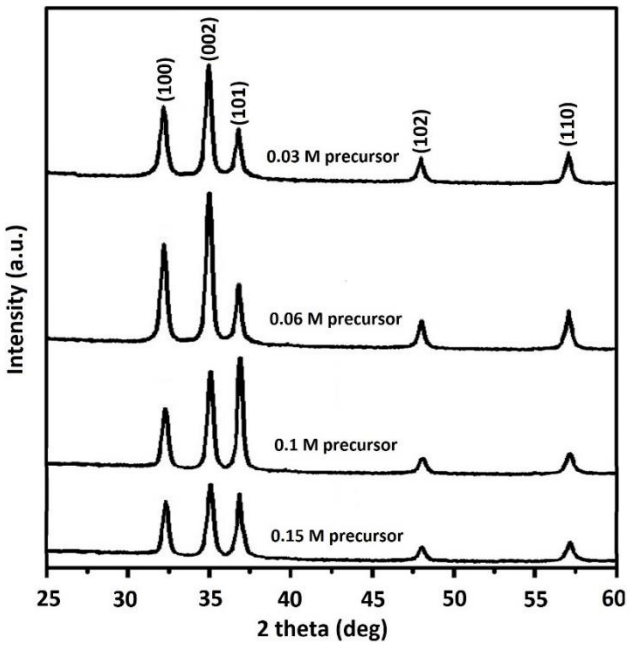

Figure 2. XRD spectra of ZnO nanostructures synthesized on the ITO/PES polymer substrates using different concentrations of precursor

X-ray diffraction (XRD) patterns of the ZnO nanorods with different concentrations of precursor are shown in Figure 2. Five pronounced wurtzite ZnO diffraction peaks, namely, (100), (002), (101), (102) and (110), appear at 2θ=31.85, 34.49, 37.26, 45.65 and 57.11, respectively. The XRD spectra of all ZnO nanorods reveal a strong (002) peak, indicating that the nanorods demonstrate high orientation with c-axis vertical to the substrate surface [18].

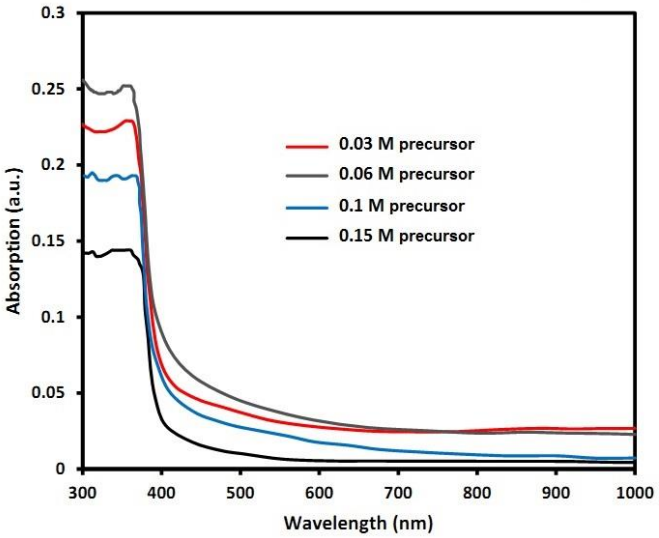

Figure 3. Optical absorption of the samples synthesized by various precursor concentrations

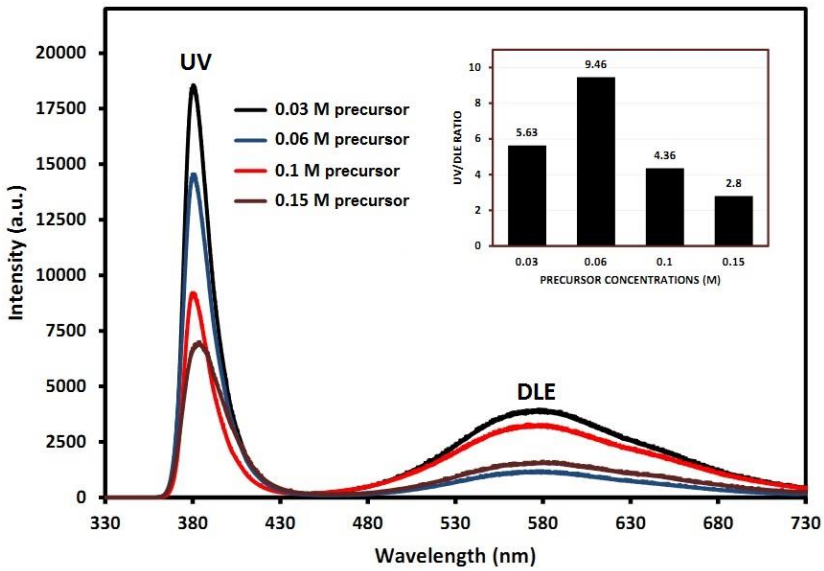

Figure 4. PL measurements of the samples grown on PES polymer substrates with various precursor concentrations. The inset indicates UV/DLE peak ratio of the samples

The optical absorption of the samples is revealed in Figure 3. As shown in figure 3, the sample B demonstrated strangely improved absorption compared to the other samples. This result shows the absorption enhancement that may be ascribed to the aspect ratio of the ZnO nanorods, which had led to

the refractive index in the regions of graded transient. Moreover, the findings can be related to the scattering of light reflection in large angles [19]. These results propose that the hydrothermally growth ZnO nanostructures with an optimum precursor concentration (0.06 M) indicate a robust light trapping effect that is valuable for photovoltaic applications.

Figure 4 indicates the PL measurements of the samples grown on PES polymer substrates with various precursor concentrations. The PL spectra reveal a sharp and strong near-band-edge (NBE) emission peak at a wavelength of about 380 nm and a wide deep-level emission (DLE) in the range of 450 nm to 730 nm. The NBE was related to the free-exciton recombination [20]. The DLE may be ascribed to structural defects and impurities in the crystal structure, for example extrinsic impurities such as O-vacancy (VO) and Zn-vacancy (VZn) [21, 22]. As shown in Fig. 4, at a low concentration of precursor, a strong and sharp enhancement in UV emission peak is observed. Furthermore, the intensity of UV emission increased three times compared to the ZnO nanorods grown at 0.15 M precursor. In contrast, the defect-related green luminescence intensity reduced, a result that indicates an improvement in the crystalline quality of the sample B. This enhancement can be mostly associated to the density and size of the ZnO nanorods. Once the diameters and size of the ZnO nanorods reduced, the surface area enhanced; both PL property and incident photon-to-current conversion efficiency were hence improved. The intensity ratio of NBE to DLE peaks for different precursor concentration indicate in the inset of Fig. 4. The NBE/DLE peak ratio is found to be maximum for 0.06 M precursor concentration sample which proposes the existence of lowest defects in ZnO nanorod crystals. The result is in good accordance with the highest light absorption obtained for sample B as shown in figure 3.

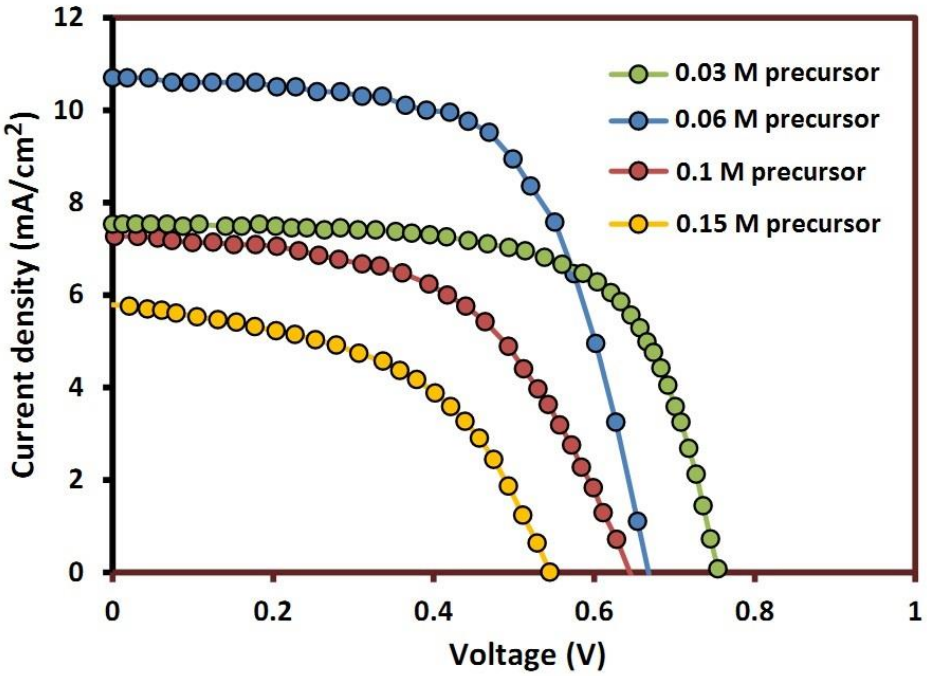

Figure 5. Current density-voltage (J-V) curves for DSSCs using the ZnO/ITO/PES as photoanodes

Figure 5 shows the stabilized current density-voltage (J-V) curves for DSSCs using the ZnO/ITO/PES as photoanodes, indicating the effect of precursor concentrations on the photoelectrochemical performances. Table 1 indicates the detailed parameters, containing the fill factor (FF), short current density (Jsc), solar conversion efficiency (η), and open circuit voltage (Voc) of the DSSCs [23]. With increasing precursor concentrations, both FF and Voc are reduced, but η and Jsc values start to increase and then decrease. Once the precursor concentrations is 0.06 M, the η and Jsc have the highest values of 4.46% and 10.73 mA/cm^2, respectively. Clearly, a proper amount of precursor significantly improve the conversion efficiency value compared to that of high amount of precursor. The Voc value is the level difference between Fermi level of absorber material and the redox potential value of I^-/I_3^- [24, 25], indicating the Voc is a constant for any given photoelectrode/electrolyte system. However, empirical results have shown that the Voc typically depends on the rate of recombination. The lower Voc with increased concentration of precursor can be clarified as a consequence of increased interfacial recombination because of the poor electron transport in the interconnected ZnO network, which results in a decrease of electron density and then the positive shift of the Fermi level [26, 27]. The fill factor were measured through the internal resistance of solar cells which decreased with the increase of the precursor concentrations because more electrons can transfer quickly by nanorod networks. Furthermore, the main reason for the large amount of Jsc are summerized in sufficient light harvesting, dye absorption and fast charge transfer.

Table 1. List of the parameter of dye-sensitized solar cells constructed by ZnO nanorods

Precursor concentration	J_{sc} (mA/cm^2)	V_{oc} (V)	FF (%)	η (%)
0.03 M (Sample A)	7.57	0.75	66.7	3.78
0.06 M (Sample B)	10.73	0.67	62.2	4.46
0.1 M (Sample C)	7.33	0.64	56.2	2.64
0.15 M (Sample D)	5.82	0.44	51.3	1.31

4. CONCLUSIONS

In this work, Well-aligned ZnO nanorods were successfully grown on ITO/PES polymer substrates using a facile aqueous solution method to study the effect of precursor concentration on photoelectrochemical and optical properties of the samples. The surface morphology of the samples was performed by FESEM. Photoelectrochemical and optical properties of the samples were done by UV–vis spectrophotometer, PL and solar simulator tests. The optical absorption revealed that the sample with 0.06 M precursor content indicated strangely improved absorption compared to the other samples which can be ascribed to the aspect ratio of the ZnO nanostructures. The PL spectra of the samples revealed a sharp and strong NBE emission peak at a wavelength of about 380 nm and a wide DLE in the range 450 nm to 730 nm. The PL results indicated an improvement in the crystalline quality of the sample (0.06 M precursor) which can be mostly associated to the density and size of the ZnO nanorods. High values of

Jsc and solar conversion efficiency were observed in the sample with 0.06 M precursor concentration which can be attributed to the sufficient light harvesting, more dye absorption and fast charge transfer of the sample.

ACKNOWLEDGEMENT
This research is supported supported by “Fundamental Research on X-ray Fluorescence CT Imaging Based on Tube Excitation Source” project of science and technology research program of Chongqing Education Commission of China.（No KJQN201904007）

References

1. J. Rouhi, C.R. Ooi, S. Mahmud and M.R. Mahmood, *Materials Letters*, 147 (2015) 34.
2. P. Shao, X. Duan, J. Xu, J. Tian, W. Shi, S. Gao, M. Xu, F. Cui and S. Wang, *Journal of hazardous materials*, 322 (2017) 532.
3. Z. Lin, Y. Wang, D. Zhang and X.-b. Li, *International Journal of Electrochemical Science*, 11 (2016) 8512.
4. R. Dalvand, S. Mahmud, J. Rouhi and C.R. Ooi, *Materials Letters*, 146 (2015) 65.
5. F. Touri, A. Sahari, A. Zouaoui and E. Deflorian, *International Journal of Electrochemical Science*, 12 (2018) 10813.
6. H. Chen, S. Zhang, Z. Zhao, M. Liu and Q. Zhang, *Progress in Chemistry*, 31 (2019) 571.
7. D. Yuan, C. Zhang, S. Tang, X. Li, J. Tang, Y. Rao, Z. Wang and Q. Zhang, *Water research*, 163 (2019) 114861.
8. M.A. Mahmud, N.K. Elumalai, M.B. Upama, D. Wang, K.H. Chan, M. Wright, C. Xu, F. Haque and A. Uddin, *Solar Energy Materials and Solar Cells*, 159 (2017) 251.
9. S. Tang, N. Li, D. Yuan, J. Tang, X. Li, C. Zhang and Y. Rao, *Chemosphere*, 234 (2019) 658.
10. S. Maiti, S. Pal and K.K. Chattopadhyay, *CrystEngComm*, 17 (2015) 9264.
11. P. Shao, J. Tian, F. Yang, X. Duan, S. Gao, W. Shi, X. Luo, F. Cui, S. Luo and S. Wang, *Advanced Functional Materials*, 28 (2018) 1705295.
12. X. He, F. Deng, T. Shen, L. Yang, D. Chen, J. Luo, X. Luo, X. Min and F. Wang, *Journal of colloid and interface science*, 539 (2019) 223.
13. L. Yang, G. Yi, Y. Hou, H. Cheng, X. Luo, S.G. Pavlostathis, S. Luo and A. Wang, *Biosensors and Bioelectronics*, 141 (2019) 111444.
14. C. Li, S. Hu, L. Yang, J. Fan, Z. Yao, Y. Zhang, G. Shao and J. Hu, *Chemistry–An Asian Journal*, 10 (2015) 2733.
15. N. Kiomarsipour and R.S. Razavi, *Ceramics International*, 40 (2014) 11261.
16. E. Ozel, I.G. Tuncolu, C. Aciksari and E. Suvaci, *Hittite Journal of Science & Engineering*, 3 (2016) 73.
17. P. Shao, L. Ding, J. Luo, Y. Luo, D. You, Q. Zhang and X. Luo, *ACS applied materials & interfaces*, 11 (2019) 29736.
18. M. Husairi, J. Rouhi, K. Alvin, Z. Atikah, M. Rusop and S. Abdullah, *Semiconductor Science and Technology*, 29 (2014) 075015.
19. S.Y. Chou and W. Ding, *Optics express*, 21 (2013) A60.
20. M.I. Dar, N. Arora, N.P. Singh, S. Sampath and S.A. Shivashankar, *New Journal of Chemistry*, 38 (2014) 4783.
21. A. Anaraki Firooz and M.H. Darvishnejad, *Inorganic and Nano-Metal Chemistry*, 47 (2017) 412.
22. N. Naderi, M. Hashim and J. Rouhi, *International Journal of Electrochemical Science*, 7 (2012) 8481.

23. A. Sedghi and H.N. Miankushki, *International Journal of Electrochemical Science*, 10 (2015) 3354.
24. M. Careem, M. Aziz and M. Buraidah, *Materials Today: Proceedings*, 4 (2017) 5092.
25. J. Rouhi, S. Mahmud, S. Hutagalung and S. Kakooei, *Micro & Nano Letters*, 7 (2012) 325.
26. G. Yang, Q. Wang, C. Miao, Z. Bu and W. Guo, *Journal of Materials Chemistry A*, 1 (2013) 3112.
27. P. Shao, J. Tian, X. Duan, Y. Yang, W. Shi, X. Luo, F. Cui, S. Luo and S. Wang, *Chemical Engineering Journal*, 359 (2019) 79.